Eng. Sci., 2021, **15**, 166–176

Engineered Science

DOI: https://dx.doi.org/10.30919/es8e506

# Dynamic Force Modelling and Experimental Analysis of Reaming

Raghavendra Kamath C,[1] Siddappa Bekinal,[1] Ritesh Bhat,[1,*] Nithesh Naik[1] and Appu Kuttan[2]

## Abstract

The production Reaming process plays a vital role in several applications, ranging from automotive to medical sectors. It is performed to enlarge the pre-drilled hole to obtain its required diameter within the specified tolerance limits. The typical operational faults found in the reaming process significantly contribute to damage in the final hole quality. Thus, a dynamic force model is developed in the present work to predict the cutting forces developed during the reaming process. The inputs to the model are broadly classified into tool geometry and vibration system elements. The cutting forces acting in all three directions during the reaming are predicted. The double modulation principle is applied to develop the dynamic force model for computing the cutting forces in the reaming process. The dynamic force model thus developed and simulated using MATLAB® R2019b is examined and validated through actual experiments for no fault conditions. The results obtained infer a high degree of fitness between the values obtained from the developed mechanistic model and the experimental values with a prediction error of less than 5%.

*Keywords:* Cutting force; Manufacturing; Mechanistic model; Reaming; Simulation; Torque.
Received: 17 July 2021; Accepted: 6 August 2021.
Article type: Research article.

## 1. Introduction

In practice, the holes are made in any component using drill tools. Reaming is performed later as a secondary operation to enlarge the pre-drilled hole to obtain its required diameter within the specified tolerance limits. A significant consideration is given to the reaming process as it plays a vital role in several applications, ranging from automotive to medical sectors.[1-3] Reaming operation ranks high amongst the finishing operation, and the tool used for reaming is known as a reamer. A reamer has several teeth and is generally made up of high-speed steel (HSS) and sintered carbide with or without coating. The typical coatings include TiN, TiC, TiCN, MT-TiCN, TiCNO, and α/K-$Al_2O_3$. Additional components and component groups extend further flexibility to coating designs, such as TiAlN, TiBN, $TiB_2$, CrCx, and $Cr_2O_3$. There exist reamers made up of other materials: polycrystalline diamond (PCD), cement, and cubic boron nitride (CBN), but they are less frequently used.[4,5] Any reamer is equipped with two or more peripheral grooves or flutes, either parallel or helix to the axis. These helical flutes provide smooth shear cutting to produce a hole close to theoretical perfection with an excellent finish.[6-7] The reamed hole finish depends on the tool's geometry and the cutting conditions. Furthermore, the typical operational faults found in the reaming process, like parallel offset runout, spindle-tilt, and axis misalignments, significantly contribute to the final hole quality. When all of the defects associated with the reaming process are examined, they all point to the effect of the cutting forces.[8-9] Thus, researchers started focusing on modelling the cutting parameters for the reaming process. In one of the experimental works, the reamed hole accuracy was investigated while using multi-fluted carbide reamers. Based on the dynamics and experimental results, the model developed highlighted that the final quality of reamed holes depends upon the relative position of the tool axis, spindle axis, and initial hole axis.[10] The applicability of the low energy conversion method on the hole-making process is discussed[11] and based on it; a mechanistic model is proposed wherein the cutting force is proved to be proportional to the chip load.[12] A mechanistic model was developed for the reaming process with a focus on process faults. The model thus developed was capable of predicting cutting forces acting on arbitrary reamer

[1] *Department of Mechanical and Manufacturing Engineering, Manipal Institute of Technology, Manipal Academy of Higher Education Manipal, Karnataka, 576104 India.*

[2] *Department of Mechanical Engineering, National Institute of Technology Karnataka (NITK), Surathkal, Mangalore, 575025 India.*

**Email:* ritesh.bhat@manipal.edu (R. Bhat)



© Engineered Science Publisher LLC 2021

geometry.[13] Another work explained the reaming cycle dynamics and their effect on the lobing pattern with a quasi-static model.[14] The experiment results followed by an analysis of variance analysis identified the grid size, reamer rotational speed, feed rate, run out of stock removal, and axial length of the specimen as the significant process variables.[15] For the reaming process, a set of researchers developed a simulation model with four parameters: cutting lips, chisel edge, dynamic model of a machine, and the regenerative association of force with machine tool vibrations. The force model is considered significant and can predict the dynamic components and limit of chatter. The authors also discussed the reason behind the effect of point angle and feed on the chatter limit.[14]

A model for cutting force in the reaming process using a time-domain approach has also been developed.[16] The dynamic analysis of the system involved tool inertia, centripetal and coriolis terms, damping, and the reamer's first mode of bending. The obtained results concluded that the incidence of chatter depends on the cutting conditions but not on the initial wave or trigger nature, which causes the tool to oscillate.[16] Later researchers also developed a 3-dimension (3D) analytical cutting force model based on the Drucker-Prager criterion for determining the cutting forces while using a single reamer cutter as the tool.[17] The model established the correlation between the cutting force and the rake angle of the reamer.[17] A work focused on developing a cutting force model for the reaming process using an experimental approach. The tool analyzed by the authors[18] was polycrystalline diamond (PCD). Results obtained proved that the cutting conditions, particularly the speed, significantly affect the cutting force.

Besides, the authors also inferred that cutting fluid changes the dynamics of the process concerning the quality of the reamed hole.[18] In recent research, a mechanistic model for cutting force in the reaming process based on the typical faults like ovality, runout and misalignment was developed, wherein a correlation between the faults and the force was successfully established.[19] From the wide range of literature reviewed concerning the reaming operation, the point understood is that most of the studies conducted are either experimental or simulation-based, involving modelling. Only a few researchers focused on employing generalized reaming process parameterization for modelling the cutting forces involved in the reaming process.

In this study, a novel approach adding to the existing literature on mechanistic modelling of the cutting forces was used to develop a dynamic force model for the reaming process to predict tangential, radial, and axial forces using proportionality constants. The inputs to this model include the mass, stiffness, and damping coefficients along with the displacements obtained from the double modulation principle. The feed is varied, and speed (control variable) is considered constant in the present work throughout the experiment. Firstly, the mechanistic modelling of cutting forces in a reaming process is discussed in further sections. The proportionality constant is determined then from the mechanistic models for the reaming process concerning different workpiece materials. This step follows the discussion regarding dynamic modelling, then the computation of dynamic forces and model parameters. The effect of input parameters is assessed further through the developed dynamic force models. Finally, the obtained results are examined by experimental validation and presented in the process's developed torque.

## 2. Theory and Calculation

### 2.1 Mechanistic cutting force model for reaming

The mechanistic approach to cutting force modelling concerning any machining process involves the fundamental equations that relate the axial force $F_x$, normal force $F_y$, and the cutting force $F_z$, to the chip cross-sectional area,[13,20] which are given by Equations (1-3):

$$F_x = P_x A_c \quad (1)$$

$$F_y = P_y A_c \quad (2)$$

$$F_z = P_z A_c \quad (3)$$

$F_x$, $F_y$, and $F_z$ are the three-dimensional forces acting at the tooltip (Newton). $A_c$ is the chip cross-sectional area ($mm^2$), and $P_x$, $P_y$, and $P_z$ are the proportionality constants corresponding to three directional cutting forces ($N/mm^2$). Besides, the cutting force proportionality constant depends on chip thickness ($t_c$), cutting velocity ($v_c$), and rake angle ($\gamma$) of the cutting tool.[13,20] Mathematically, $P_x$, $P_y$, and $P_z$ are shown as Equations (4-6):

$$log\, P_x = a_0 + a_1\, log\, t_c + a_2\, log\, v_c + a_3\, log\, t_c\, log\, v_c + a_4\, log\, \gamma_a \quad (4)$$

$$\log P_y = b_0 + b_1 \log t_c + b_2 \log v_c + b_3 \log t_c \log v_c + b_4 \log \gamma_a \quad (5)$$

$$\log P_z = c_0 + c_1 \log t_c + c_2 \log v_c + c_3 \log t_c \log v_c + c_4 \log \gamma_a \quad (6)$$

The coefficients $a_i$, $b_i$, and $c_i$ (i = 1, 2, 3, 4) are the specific cutting energy constants. The constants are dependent on the tool geometry, the workpiece material, the range of cutting speed, and the chip thickness. The coefficients are, however, independent of the machining process. Usually, these constants are determined by the calibration test for the combination of the tool and the workpiece and by a range of cutting conditions.

### 2.2 Proportionality constants for reaming operation

Proportionality constants concerning the cutting force and the chip area obtained are the results of the experiment. The proportionality constants are functions of workpiece material and tool geometry but are independent of the cutting process. Thus, the proportionality constants determined in specific cutting constants for reaming operation are from the drilling process. The method is advantageous for the dynamic modelling of the cutting forces, particularly for reaming operations. The drill bit used for the calibration test exhibited the reamer geometry (gauged using a toolmaker microscope). The present work used three different reamers, *i.e.*, 15, 20, and 24 mm in diameter. For the calibration purpose, initially, 14.5, 19.5 and 23.5 mm holes are made using conventional twist

© Engineered Science Publisher LLC 2021

drill and then enlarged to 15, 20, and 24 mm using the reamer-geometry equivalent drill bits to measure the three-dimensional cutting forces. A linear graph plotted using the linear curve fitting method is used for determining the cutting force against the chip thickness data obtained during the experiments. The linear curve is obtained by using MATLAB® R2019b software. Table 1 gives the specific cutting constants values determined from the linear curve for two different materials: mild steel and aluminium.

**Table 1.** The experimental values of specific cutting constants.

| Material | $c_0$ | $c_1$ | $b_0$ | $b_1$ | $a_0$ | $a_1$ |
|---|---|---|---|---|---|---|
| Aluminum | 2.26 | 0.10 | 4.1 | 0.84 | 5.08 | 0.9 |
| Mild steel | 4.2 | 0.76 | 4.2 | 0.85 | 5.21 | 0.92 |

In the calibration test, the tool's rake angle (γ) and cutting velocity (v) were constant. Therefore, the proportionality constants Px, Py, and Pz depend only on the chip thickness (tc) in the present work. Thus, Equations (4), (5), and (6) in their reduced form are given by:

$$log\, P_x = a_0 + a_1\, log\, t_c \quad (7)$$

$$log\, P_y = b_0 + b_1\, log\, t_c \quad (8)$$

$$log\, P_z = c_0 + c_1\, log\, t_c \quad (9)$$

wherein, $t_c$, measured, is from the chip curl collected during the experiments. The chip curl volume is determined using the water volume displacement method and the width by a micrometre. Table 2 gives the values of the proportionality constants thus obtained from Equations (7), (8), and (9).

**Table 2.** Proportionality constants for the reaming process from the model.

| Material | Px (N/mm2) | Py (N/mm2) | Pz (N/mm2) |
|---|---|---|---|
| Aluminium | 107.13 | 146.93 | 1020.94 |
| Mild steel | 309.03 | 175.44 | 1238.94 |

### 2.3 Dynamic Model

Knowing the cutting forces and torque on a tool, a dynamic model for any machining process could be developed. The cutting force information is useful for designing reamer and machine tools and reducing the tool wear and breakage. The cutting force attributes of machine tool vibration are dominant with run out, reamer geometry defects, and misalignments. An initial disturbance to the machine tool system due to static load acting on the reamer leads to a relative displacement between tool and workpiece. The self-weight of the machine components and inertial effect due to the mass of the components are the prime reasons for the discussed disturbance. The relative displacement between the tool and the workpiece induces vibration, and subsequent machining results in varying chip thickness, resulting in a dynamic force component. The dynamic force component, along with static force, leads to the development of regenerative vibration. The dynamic force models are formulated on the following assumptions.[20]

- The static cutting forces $F_x$, $F_y$, and $F_z$, begin to excite the stationary reaming machine. The static force analysis includes the Computation of instantaneous X, Y, and Z components of the reamer rotation angle (ϕ). It is the sum of all simultaneously engaged cutting points.
- The regenerative vibration generates dynamic cutting forces. Thus, it attributes to the dynamic force component. However, for heavy cutting conditions and machining the hard materials, it does not yield satisfactory results.

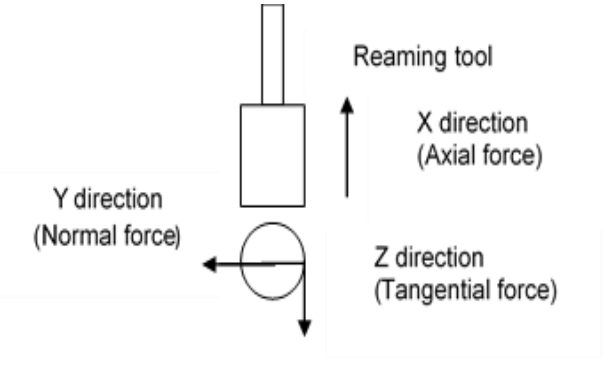


**Fig. 1** Diagram showing the direction of the cutting forces acting on a reamer.

Dynamic forces are developed mainly due to the chip thickness variation during the reaming operation. Fig. 1 shows the directions of the developed forces acting on the reamer during reaming, and Fig. 2 illustrates the various angles corresponding to the chip edges of the reamer. The theory of double modulation induces variations in the chip thickness during machining,[21] which is defined by the internal modulation corresponding to the relative displacement of the system and by the external modulation determined by the internal modulation due to the rotational speed of the reamer and the number of tool cutting edges. For simplicity, to understand the dynamic system, two degrees of freedom in X-direction are assumed for both workpiece and tool with instantaneous inner modulation of the $t^{th}$ cutting edge of the reamer at the rotation angle $\varphi$ and given by,

$$X_I(t,\varphi) = X_1(t,\varphi) - X_2(t,\varphi) \quad (10)$$

$X_1$ and $X_2$ represent the tool and workpiece displacements corresponding to the reamer rotational angle (φ), respectively. Delaying the inner modulation caused due to the time lag of one tip of the reamer determines the instantaneous outer modulation $X_0$ (t, φ), which is given by Equation (11):

$$X_0(t,\varphi) = X_I\left[t, \left(\varphi - \frac{2\pi N}{60 Z_n}\right)\right] \quad (11)$$

$Z_n$ is the total number of cutting edges, and N is the operating speed of the reamer. The product of cutting force coefficient $K_n$ and incremental chip thickness variation ($Ux\,(t,\varphi)$) defines the instantaneous dynamic force component $dF_X$ (t, φ) in the X-direction at a reamer rotation angle φ[21] given by Equation (12):

$$dF_X(t,\varphi) = K_n\, Ux\,(t,\varphi) \quad (12)$$

wherein, $Ux\,(t,\varphi) = [X0\,(t,\varphi) - XI\,(t,\varphi)]$ is the


© Engineered Science Publisher LLC 2021

incremental chip thickness variation, and $K_n$ is the complex frequency-dependent quantity. However, for simplicity, the value of $K_n$ is considered as the average value of static specific cutting constants. Further, assuming a unit chip thickness, the resultant force $DF_X$ with a dynamic force ($dF_X(t,\varphi)$) and static force ($F_X(t,\varphi)$) is given by Equation (13):

$$DF_X(t,\varphi) = F_X(t,\varphi) + dF_X(t,\varphi) \quad (13)$$

Similarly, the formulation of dynamic force extends to the three-dimensional considerations. Let $R_X$ (t, φ), $R_Y$ (t, φ), and $R_Z$ (t, φ) be the incremental chip thickness in the X, Y and Z directions, then the three-dimensional resultant force $dF_X$ (t, φ), $dF_Y$ (t, φ) and $dF_Z$ (t, φ) in three directions cartesian coordinate system is obtained as Equation (14):

$$\begin{bmatrix} U_X \\ U_Y \\ U_Z \end{bmatrix} = \begin{bmatrix} G_{XX} & G_{XY} & G_{XZ} \\ G_{XX} & G_{XY} & G_{XZ} \\ G_{XX} & G_{XY} & G_{XZ} \end{bmatrix} \begin{bmatrix} dF_X \\ dF_Y \\ dF_Z \end{bmatrix} \quad (14)$$

where,

$$G_{pq}(t,\varphi) = \frac{R_p(t,\varphi)}{dF_q(t,\varphi)} \text{ and } p,q = X,Y,Z \quad (15)$$

Equation (15) gives the ratio of the incremental chip thickness variations to resultant cutting force. The dynamic cutting force for any particular degree of freedom could be determined by knowing the model parameters of the machine tool system. The worktable and machine tool spindle heads are assumed to be rigid. As a result, the vibratory system is modelled as six degrees of freedom system.

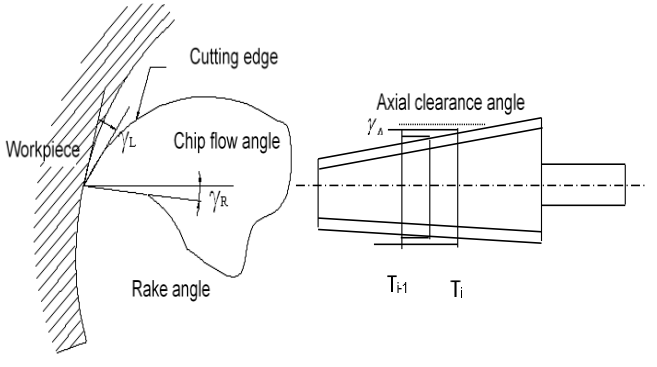


**Fig. 2** The rake angle, chip flow angle, and the lead angle of the reamer.

Assuming the tool and workpiece as a rigid body,[21] the three-dimensional vibratory model for reaming shown in Fig. 3 is modelled as Equation (16):

$$[M]\{\ddot{X}\} + [C]\{\dot{X}\} + [K]\{X\} = [F] \quad (16)$$

wherein, $[F] = [F_X\ 0\ F_Y\ 0\ F_Z\ 0]^T$ is the force vector and $\{X\} = [x_1\ x_2\ y_1\ y_2\ z_1\ z_2]^T$ is the relative displacement vector between tool and workpiece. $[M]$ is the mass matrix that depends on the tool and the workpiece, $[C]$ is the damping coefficient between the tool and workpiece, which depends on cutting speed and feed, and $[K]$ is the stiffness matrix connecting the tool and the workpiece.[21] Considering Fig. 3, the vibration model parameters for reaming operation is given by Equation (17):

$$[M] = \begin{bmatrix} M_1 & 0 & 0 & 0 & 0 & 0 \\ 0 & M_2 & 0 & 0 & 0 & 0 \\ 0 & 0 & M_1 & 0 & 0 & 0 \\ 0 & 0 & 0 & M_2 & 0 & 0 \\ 0 & 0 & 0 & 0 & M_1 & 0 \\ 0 & 0 & 0 & 0 & 0 & M_2 \end{bmatrix} \quad (17)$$

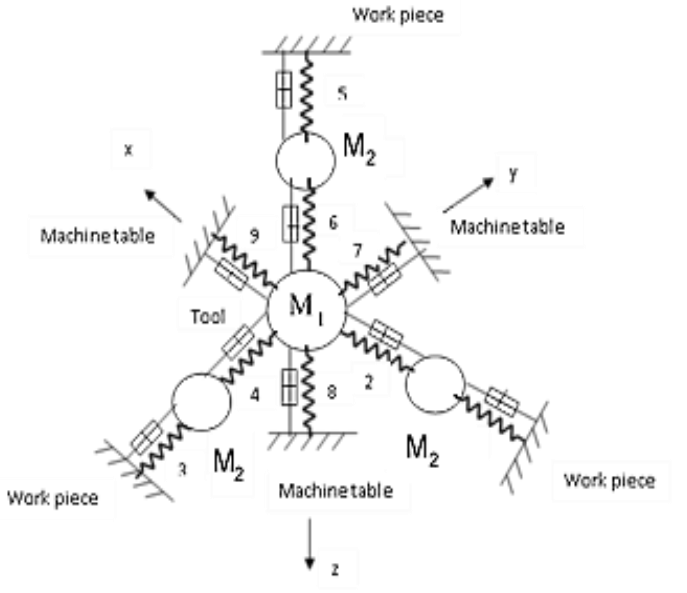


**Fig. 3** Three-dimensional vibratory models for the reaming operation.

Table 3 gives the parameters corresponding to the system stations indicated in Fig. 3. The x, y, and z suffixes in matrices are also noted by suffixes 1, 2, and 3, respectively, for the formulation. Equations (18) and (19) represent the matrix $[C]$ and $[K]$ while considering the given parameters.

**Table 3.** Parameters corresponding to the system with six degrees of freedom.

| Stations | 1 | 2 | 3 | 4 | 5 | 6 | 7 | 8 | 9 |
|---|---|---|---|---|---|---|---|---|---|
| Spring constant | $K_{13}$ | $K_{12}$ | $K_{23}$ | $K_{22}$ | $K_{33}$ | $K_{23}$ | $K_{21}$ | $K_{31}$ | $K_{11}$ |
| Damping coefficient | $C_{13}$ | $C_{12}$ | $C_{23}$ | $C_{22}$ | $C_{33}$ | $C_{23}$ | $C_{21}$ | $C_{31}$ | $C_{11}$ |

$$[C] = \begin{bmatrix} C_{11}+C_{12} & -C_{12} & 0 & 0 & 0 & 0 \\ -C_{12} & C_{12}+C_{13} & 0 & 0 & 0 & 0 \\ 0 & 0 & C_{21}+C_{22} & -C_{23} & 0 & 0 \\ 0 & 0 & -C_{23} & C_{23}+C_{31} & 0 & 0 \\ 0 & 0 & 0 & 0 & C_{31}+C_{32} & -C_{32} \\ 0 & 0 & 0 & 0 & -C_{32} & C_{32}+C_{33} \end{bmatrix} \quad (18)$$

$$[K] = \begin{bmatrix} K_{11}+K_{12} & -K_{12} & 0 & 0 & 0 & 0 \\ -K_{12} & K_{12}+K_{13} & 0 & 0 & 0 & 0 \\ 0 & 0 & K_{21}+K_{22} & -K_{23} & 0 & 0 \\ 0 & 0 & -K_{23} & K_{23}+K_{31} & 0 & 0 \\ 0 & 0 & 0 & 0 & K_{31}+K_{32} & -K_{32} \\ 0 & 0 & 0 & 0 & -K_{32} & K_{32}+K_{33} \end{bmatrix} \quad (19)$$

Using the Wilson Theta Method[21] earlier discussed in Equations (10) and (11), the deflection in X(t), Y(t), and Z(t) for the time interval (Δt) is computed. For the first iteration, the forces $F_X$, $F_Y$, $F_Z$ are obtained using the static analysis as given in Equations (1), (2) and (3), later the displacement vector {X} is computed using Equation (16). Knowing the values of the vector {X}, inner and outer modulations are computed. Knowing the inner modulation and outer modulation, $U_X(t,\varphi)$, $U_Y(t,\varphi)$, and $U_Z(t,\varphi)$ are computed using Equation (14).

Knowing $U_X(t,\varphi)$, $U_Y(t,\varphi)$, and $U_Z(t,\varphi)$, the resultant displacement of chip thickness variation is obtained by Equation (20):

$$U(t,\varphi) = \sqrt{U_X(t,\varphi)^2 + U_Y(t,\varphi)^2 + U_Z(t,\varphi)^2} \quad (20)$$

Equation (12) is extended to compute instantaneous dynamic force components in three directions $dF_X(t,\varphi)$, $dF_Y(t,\varphi)$ and $dF_Z(t,\varphi)$ for the time interval (Δt), caused by total chip thickness variation $U(t,\varphi)$ as Equations (21-23):

$$dFx\,(t,\phi) = Px\;U(t,\phi) \quad (21)$$

$$dFy\,(t,\phi) = Py\;U(t,\phi) \quad (22)$$

$$dFx\,(t,\phi) = Pz\;U(t,\phi) \quad (23)$$

wherein, $P_x$, $P_y$, and $P_z$ are known as proportionality constants which are determined experimentally. PX, PY, and PZ values are obtained by drilling calibration tests for a particular material and process condition. From the analysis, the observation is that the radial force is small compared to the tangential force. Dynamic forces $dF_x$, $dF_y$, and $dF_z$ are then determined. The calculated dynamic forces are used in the next iteration to solve Equation (16). The process is continued until convergence occurs. The Wilson-theta method is a linear multistep method for second-order equations. In the Wilson Theta approach, the fundamental assumption is that the acceleration varies linearly with time for a moment and over an extended period or phase. The computation is performed at each interval of time.[22] Since reaming is a slow process, the Wilson theta method is adopted.

## 3. Material and methods

### 3.1 Experimental setup

The machine tool used in the present work is Deckel Maho DMU 60, a universal milling and drilling machine. Cutting forces are measured using a three-component Kistler® 9257 dynamometer. Other used elements in the experimental setup are a charge amplifier, two analogue peak indicators, connecting wires, collets, and drills (geometry equivalent to reamer).

Fig. 4 shows the clamping arrangement for the conducted experimental operations. Table 4 gives the specification of DMU 60.

The experimental procedures involve drilling the workpieces with a conventional twist drill of 14.5, 19.5, and 23.5 mm to precisely locate the centre of the drilled hole. Later 15, 20 and 24 mm drills with a geometry similar to the reamer under investigation are used to enlarge and give a finishing touch. The force data gathered from the secondary drilling (equivalent to the reaming operation) is considered for calibration and validation of the proposed mechanistic model.

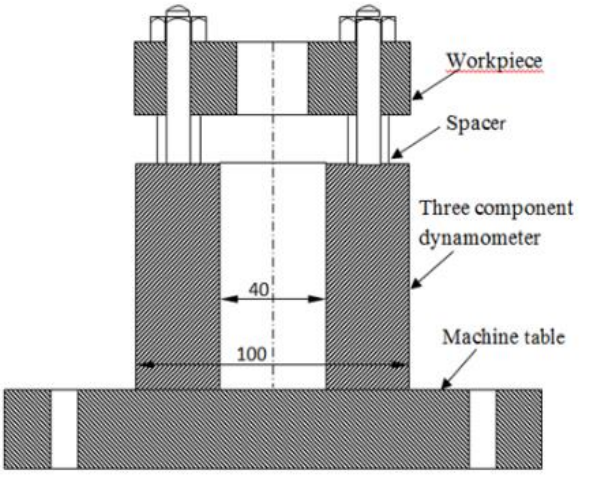


**Fig. 4** Clamping arrangement of the workpiece.

**Table 4.** Technical specification of DMU 60.

| Parameters | Specification |
|---|---|
| Feature used | Rigid reaming cycle |
| Control system | Heidenhein TNC 430 |
| Table size | NC rotary table (c-axis) , dia. 350 x 510 mm |
| Table loading capacity | 300 Kgs. |
| Axis traverse | x-axis: 600 mm; y-axis: 520 mm; z-axis: 500 mm |
| Spindle speed | 20 to 6300 rpm |
| Motor power | 13 kW |
| Table | Three axes - x, z and c |
| Spindle | One axis – y |

### 3.2 Computation of dynamic forces

Dynamic forces generated are due to the chip thickness variation. Thus for the computation of dynamic forces, the static forces acting on the reamer are resolved into global coordinates (workpiece coordinates). Consider the 15 mm reamer. 14, 20, and 8º, respectively, are the estimated cutting angles γR, γL, and γA.

The cutting speed for the power tool reaming is kept constant at 400 rpm. The static forces are measured

 © Engineered Science Publisher LLC 2021

experimentally with the Kistler®9257 dynamometer in all three directions. The cutting forces acting on the workpiece coordinates are Fx = 245.8304 N, Fy = 12.9823 N, Fz = 41.7644 N, and that at the tooltip coordinate are Fx = 228.15 N, Fy= 90.80 N, and Fz = 45.63 N. It can be inferred that there is not much difference in the cutting force between tooltip coordinate and global coordinate values, variation in the radial force with tooltip coordinate system is significant. In initial iterations, static forces obtained in tool coordinate (Fx = 228.15 N, Fy = 90.80N and Fz = 45.63 N) are used as the input force. For dynamic analysis, the numerical integration method is used to solve the Equation (16). Dynamic force values obtained from the latest displacements X, Y, and Z and new relative displacements Ux, Uy, and Uz are computed in the next iteration. The total forces are calculated by the superposition of static and the latest dynamic components. Thus, the instantaneous total force at reamer angle φ, namely $DF_X$, $DF_Y$, and $DF_Z$ is obtained by adding the static force components $F_X$, $F_Y$, $F_Z$, and dynamic force components $dF_X$, $dF_Y$, dFz as,

$$\begin{bmatrix} DF_X \\ DF_Y \\ DF_Z \end{bmatrix} = \begin{bmatrix} F_X \\ F_Y \\ F_Z \end{bmatrix} + \begin{bmatrix} dF_X \\ dF_Y \\ dF_Z \end{bmatrix} \quad (24)$$

### 3.3 Computation of dynamic model parameters

The determination of the natural frequency of the reamer is essential to determine the parameters for the dynamic force computation model. The reaming machine tool spindle is a heavy cylindrical shaft with a natural frequency of around 400 Hz. Hence, only the reamer configuration is considered for determining the torsional frequency.

Assuming reamer as a thin shaft with a mass moment of inertia $I_\omega$ is, we have

$$I_\omega = \frac{M_1 d^2}{8} \quad (25)$$

where, '$M_1$' is the mass, 'd' is the diameter and 'Kt' is the stiffness of the reamer obtained by Equation (26):

$$K_t = \frac{T}{\theta} = \frac{GJ}{L} \quad (26)$$

$T$ is the applied torque, $\theta$ is the angular twist, $G = 0.8\times10^5$ N/mm$^2$ is the modulus of rigidity, $L$ is the length of the reamer, and $J = \pi d^4/32$ is the polar moment of inertia. Considering the hub and spindle, the reamer is taken as a stepped shaft. The equivalent stiffness is computed considering the stiffness of each stepped shaft connected in series. Equivalent torsional stiffness $K_{eq}$ can be computed as Equation (27):

$$\frac{1}{K_{eq}} = \frac{1}{K_{t1}} + \frac{1}{K_{t2}} \quad (27)$$

$K_{t1}$ is the stiffness of the spindle, and $K_{t2}$ is the stiffness of the hub, and $J_1$ and $J_2$ are the corresponding polar moment of inertia for the spindle and hub. Hence, assuming the mass of the reamer as a lumped mass, the natural frequency ($\omega_n$) of the system is given by Equation (28):

$$\omega_n = \sqrt{\frac{K_{eq}}{I_\omega}} \quad (28)$$

Table 5 gives the Numerical values for the computation of the $\omega_n$ for different reamers and various components such as equivalent stiffness, the moment of inertia, and the mass moment of inertia for different reamer sizes.

To determine the dynamic forces using Equation (10), mass matrix [$M$], damping coefficient [$C$], and stiffness [$K$] have to be determined. The parameters for the dynamic system are determined from the damped natural frequency obtained experimentally from the force spectrum and the theoretically determined natural frequency of the reamer. The damped natural frequency is computed from the experimentally obtained data and the natural frequency of the reamer.

**Table 5.** Natural frequencies of the reamer for different sizes.

| Parameter | Numerical values | | |
|---|---|---|---|
| Reamer size | 24 mm | 20 mm | 15 mm |
| Mass | 0.719 | 0.399 | 0.259 |
| Diameter | 24 | 20 | 15 |
| Length of cutter | 71.52 | 54.82 | 54 |
| Length of shank | 93.56 | 97.46 | 75.5 |
| Diameter of shank | 21.46 | 17.38 | 13.84 |
| $J_1$ | 32576.25 | 15710 | 4970.74 |
| $J_2$ | 20824.52 | 8958.92 | 3602.47 |
| $Kt_1$ | 36438765.1 | 22925939.4 | 7364062.5 |
| $Kt_2$ | 17806347.59 | 7353919.48 | 3817188.42 |
| $Kt_e$ | 11961286.19 | 5567909.45 | 2514031.24 |
| $I_\omega$ | 51.768 | 19.95 | 7.284375 |
| $\omega_n$ | 480.682 | 528.293 | 587.475 |

It is well known that damped natural frequency ($\omega_d$) is given by Equation (29):

$$\omega_d = (\sqrt{1-\zeta^2})\omega_n \quad (29)$$

where, $\zeta$ is the damping ratio and $\omega_n$ is the natural frequency. Considering a lumped mass system in three directions and since the used reamer has three flutes, the mass of reamer of 15 mm diameter is $M_1$ = 0.259 kg and hence $M_2 = M_1/3$ = 0.086 kg. Then, from the typical experimental force spectrum obtained for the above reamer, the period for dynamic force is $T$=0.017 seconds. Hence, the damped natural frequency $f_d$=1/T is equal to 57.99 cycles/sec. Hence, the value of $\omega_d = 2\pi f_d$ is 364.18 radians/sec. Since the natural frequency of the 15 mm reamer is 587.4 radians/sec, the damping factor $\zeta$ is equal to 0.78. Since $k_{11}$= 7.3 × 10$^6$ N/mm and $c_{11}$ = 150 N/mm/sec. Similarly, all the parameters of Equation (16) are determined. Table 6 gives the values of the computed model parameters for dynamic cutting force analysis.

Using the mass parameters, stiffness parameters, and damping coefficients, the mass matrix, stiffness matrix, and damping coefficient matrix are obtained using Equations (17), (18) and (19). Knowing the values of the mass matrix, damping coefficient matrix, stiffness matrix, and force vector, the relative displacement between the tool and workpiece is computed using Equation (20). The computed mass, stiffness, and damping coefficient matrix are given by Equations (30-32):

© Engineered Science Publisher LLC 2021

$$[M] = \begin{bmatrix} 0.259 & 0 & 0 & 0 & 0 & 0 \\ 0 & 0.086 & 0 & 0 & 0 & 0 \\ 0 & 0 & 0.259 & 0 & 0 & 0 \\ 0 & 0 & 0 & 0.086 & 0 & 0 \\ 0 & 0 & 0 & 0 & 0.259 & 0 \\ 0 & 0 & 0 & 0 & 0 & 0.086 \end{bmatrix} \quad (30)$$

$$[K] = \begin{bmatrix} 13.3 & -6.0 & 0 & 0 & 0 & 0 \\ -6.0 & 13.3 & 0 & 0 & 0 & 0 \\ 0 & 0 & 12.8 & -6.8 & 0 & 0 \\ 0 & 0 & -6.8 & 12.8 & 0 & 0 \\ 0 & 0 & 0 & 0 & 13.3 & -6.0 \\ 0 & 0 & 0 & 0 & -6.0 & 13.3 \end{bmatrix} 10^6 \quad (31)$$

$$[C] = \begin{bmatrix} 150 & -50 & 0 & 0 & 0 & 0 \\ -50 & 60 & 0 & 0 & 0 & 0 \\ 0 & 0 & 150 & -10 & 0 & 0 \\ 0 & 0 & -10 & 110 & 0 & 0 \\ 0 & 0 & 0 & 0 & 150 & -50 \\ 0 & 0 & 0 & 0 & -50 & 60 \end{bmatrix} \quad (32)$$

**Table 6.** Damping coefficients and stiffness parameters for the dynamic model.

| Damping coefficients | Damping coefficient Value (N/mm-sec) | Stiffness parameters | Stiffness parameter Value (N/mm) |
|---|---|---|---|
| $c_{11}$ $c_{21}$ $c_{31}$ | 150 | $k_{11}$ $k_{31}$ $k_{13}$ | $7.3 \times 10^6$ |
| $c_{12}$ $c_{22}$ $c_{32}$ | 50 | $k_{12}$ $k_{22}$ $k_{32}$ | $6.0 \times 10^6$ |
| $c_{13}$ $c_{23}$ $c_{33}$ | 150 | $K_{21}$ $k_{23}$ $k_{33}$ | $6.8 \times 10^6$ |

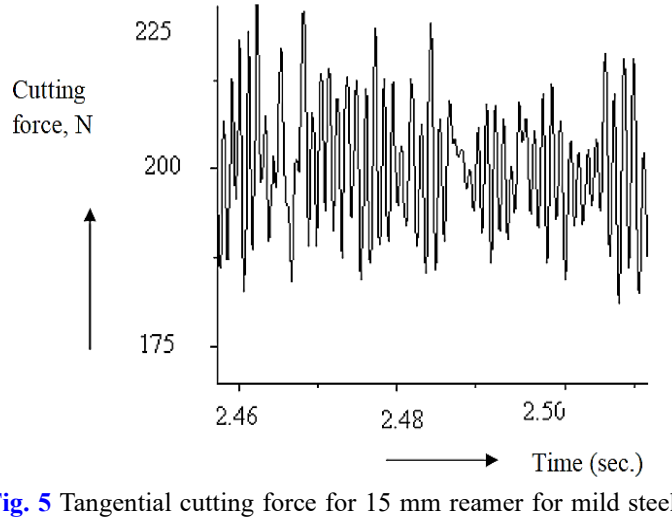


**Fig. 5** Tangential cutting force for 15 mm reamer for mild steel workpiece.

## 4. Results and Discussion

Fig. 5 shows the steady-state tangential force spectrum obtained during the power tool reaming operation for the 15 mm reamer on the mild steel workpiece. The force spectrum indicates the dynamics of the cutting forces during the power tool reaming. In other words, the force spectrum indicates the development of the cutting forces as a function of time for the specified tool geometries and the cutting conditions used. Force spectrum results from the algorithms based on discrete fourier transforms (DFT) to compute the cutting forces. Since the cutting forces are assumed to be periodic, the (root-mean-square) RMS spectrum is established, and the RMS values of the cutting force are computed. This is a proven method by researchers to determine and quantify the cutting forces in a machining process.[23-24]

Using the discussed RMS approach, the cutting forces: tangential, radial and axial forces, for 15, 20 and 24 mm diameter reamer while machining mild steel and aluminium are computed. Table 7 gives the thus calculated RMS values quantifying the different cutting forces calculated for different reamer sizes obtained while machining mild steel and aluminium.

**Table 7**. Experimentally obtained three directional cutting forces.

| Workpiece | Reamer size (mm) | RMS values of the cutting forces from the experiment | | |
|---|---|---|---|---|
| | | Tangential force ($F_z$) N | Radial force ($F_y$) N | Axial force ($F_x$) N |
| Mild steel | 15 | 218.43 | 53.61 | 3.80 |
| | 20 | 236.79 | 61.21 | 4.91 |
| | 24 | 247.13 | 82.61 | 5.01 |
| Aluminum | 15 | 128.24 | 18.25 | 4.55 |
| | 20 | 141.47 | 23.19 | 6.50 |
| | 24 | 199.78 | 37.56 | 9.25 |

The experimental results indicate that the cutting force variations are observed with variation in the reamer size. However, there is no variation in the cutting forces due to variation in the speed of reaming operation, further enhanced by comparing the results against the cutting forces obtained through manual reaming. The phenomenon agrees with an observation made by Yang *et al.*[25] in their research, wherein the cutting force varied with the variance in the diameter, irrespective of the cutting speed. Fig. 6 (a) shows experimentally obtained torque values for mild steel material for 15, 20 and 24 mm reamer diameter. The graph clearly

 © Engineered Science Publisher LLC 2021

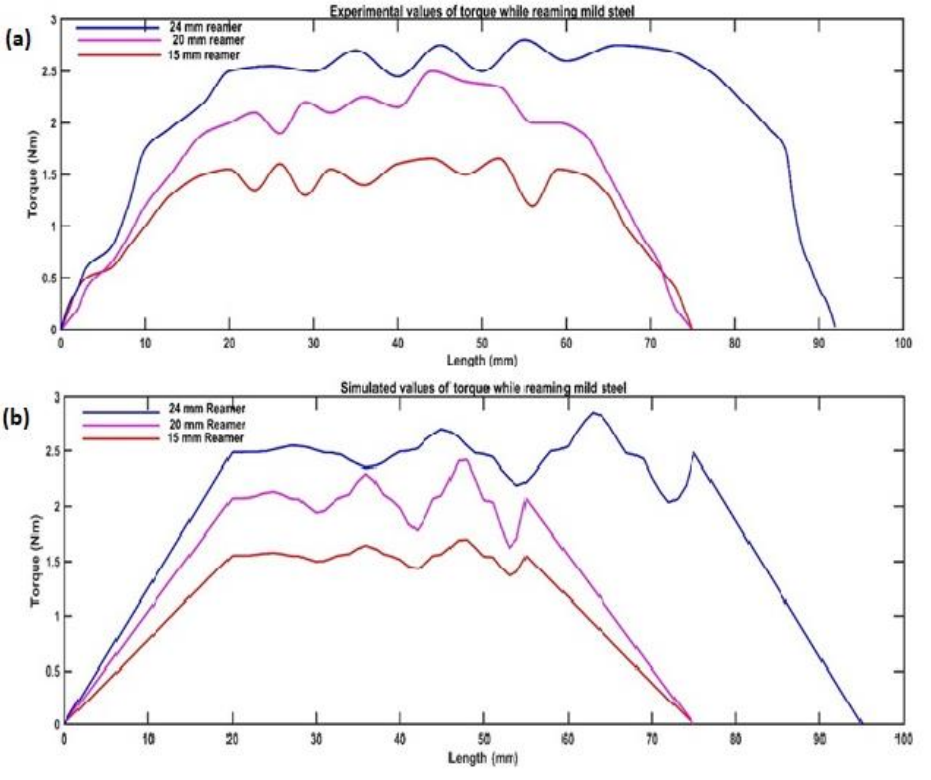


**Fig. 6** (a) Experimental values (b) Simulated values of torque while reaming mild steel with 15, 20 and 24 mm diameter reamer.

shows that the torque requires a linear increase without any dynamic force as the reamer enters the workpiece. The dynamic force behaviour is indicated when the reamer fully engages the workpiece until the reamer disengages. The dynamic force is 1.6% to 2% of the static force in all cases.

Fig. 6 (b) shows the simulated results of cutting torque required for reaming mild steel workpiece for different sizes of the reamers such as 15, 20, and 24 mm. It also shows the dynamics of the cutting process.

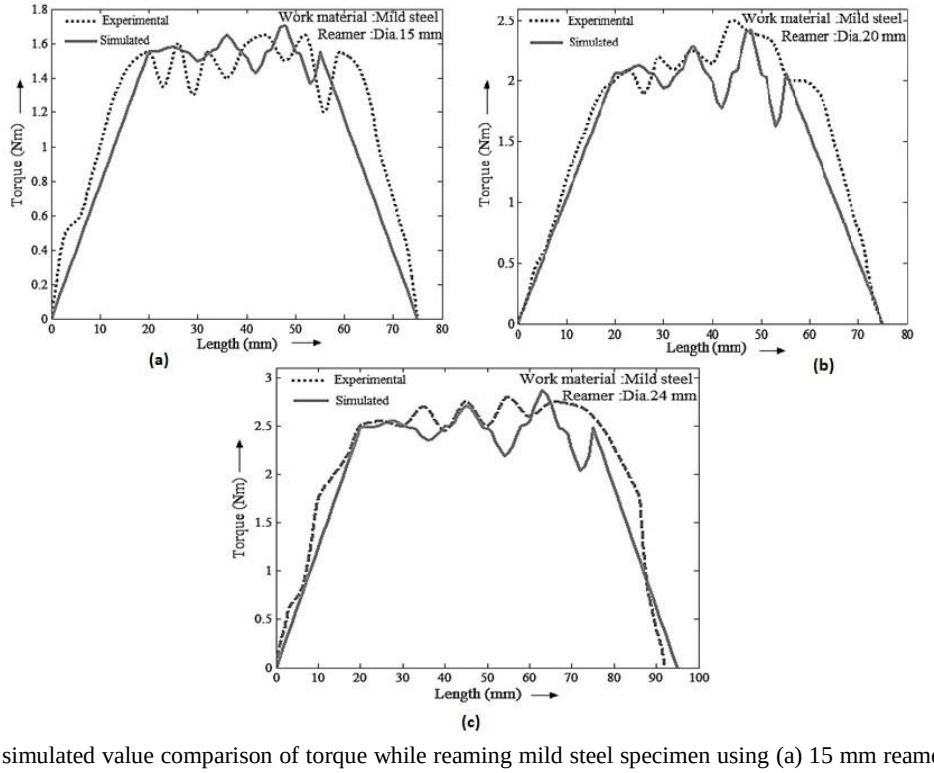


**Fig. 7** Experimental and simulated value comparison of torque while reaming mild steel specimen using (a) 15 mm reamer (b) 20 mm reamer (c) 24 mm reamer.

© Engineered Science Publisher LLC 2021

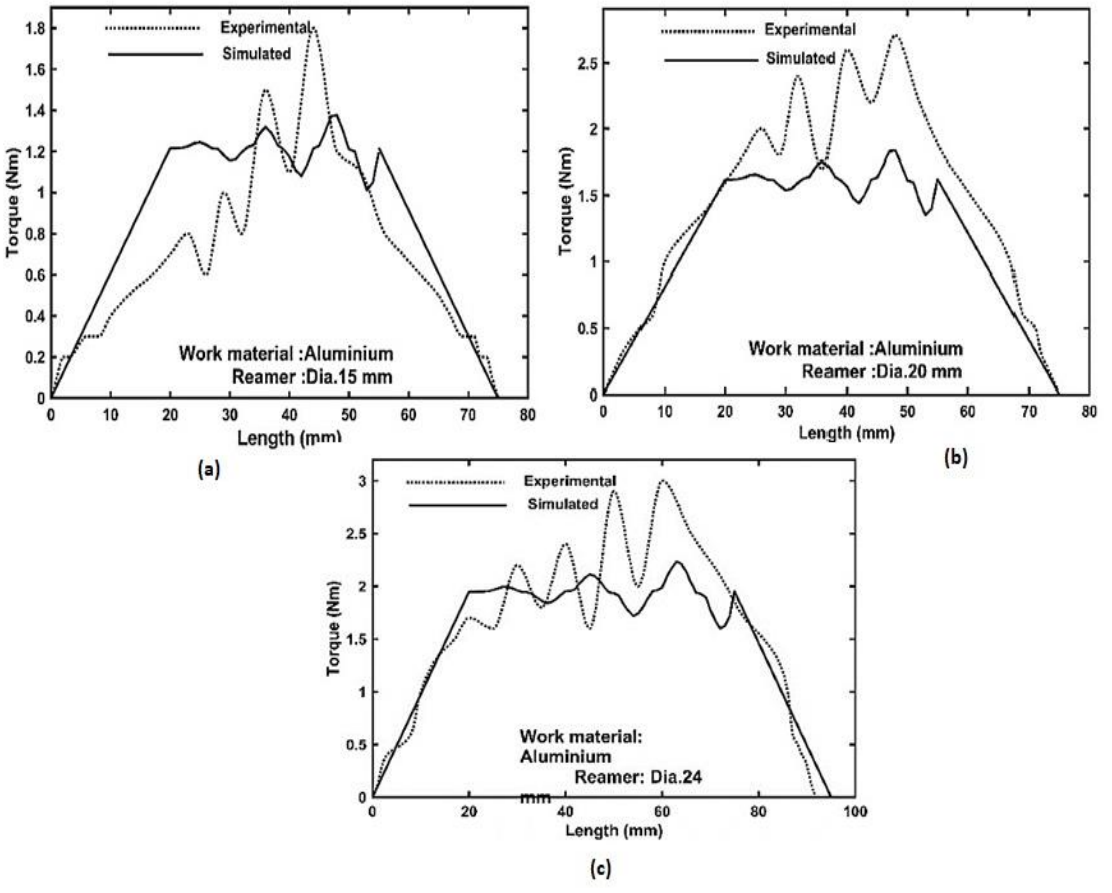


**Fig. 8** Experimental and simulated value comparison of torque while reaming aluminium specimen using (a) 15 mm reamer (b) 20 mm reamer (c) 24 mm reamer

When the size of the reamer is increased accordingly, the necessary static cutting force is also increased. However, there is no significant change in dynamic forces. The change in dynamic forces is primarily due to the variation of the cutting chip during the reaming operation. It is obvious that as the reamer diameter is increased, the cutting force is also increased.

Fig. 7 compares simulated (model) torque values with the experimental results for the mild steel workpiece considering 15, 20 and 24 mm diameter reamers, respectively. Fig 8 compares the simulated (model) torque values with the experimental results for the aluminium workpiece for 15, 20 and 24 mm diameter reamers. From the figures, at most of the points, it could be observed that the simulated results agree with the experimental results. However, in some cases, the experimentally obtained cutting forces are 2 to 10% higher than simulated results, which may be due to the addition of certain additional forces resulting from the deflection of the reamer towards the initial hole axis[26] caused by the operational faults like the run out, ovality, or misalignment.

## 5. Conclusions

Reaming is a critical operation concerning several assembly processes. The typical operational faults found in the reaming process, like parallel offset runout, spindle-tilt, and axis misalignments, significantly contribute to the final hole quality. The present work reports the dynamic force modelling of the reaming process developed using MATLAB® R2019b to minimize the defects by predicting the cutting forces accurately. The developed model is well validated concerning the computation of tangential force and torque values with experimental results for different reamer sizes on different materials, including mild steel and aluminium. The experiment has been carried out using a Deckel Maho DMU60, universal milling and drilling machine for the mild steel and aluminium material using reamers of size 15, 20, and 24 mm. The following conclusions are drawn from the work.

- The tool geometry and vibrational system components are parameterized, and the factors affecting the cutting forces (*i.e.*, tangential, axial, and radial) are identified. Various tool geometries considered include diameter, tool shank length, tool cutter length, and shank diameter. The vibration system components comprise the mass of the tool, equivalent stiffness, and damping coefficients.
- The double modulation principle is applied to develop the dynamic force model for computing the cutting forces in the reaming process, wherein the holes are initially drilled using a conventional high-speed steel twist drill of 14.5, 19.5 and 23.5 mm diameter and then

 © Engineered Science Publisher LLC 2021

reamed using a reamer geometry with an equivalent drill of 15, 20 and 24 mm diameter.

- The dynamic force model developed and simulated using MATLAB® R2019b is examined and validated through actual experiments for no fault conditions. The results obtained infer a high degree of fitness between the developed mechanistic model and the experimental value with less than 5% prediction error.
- The values obtained from the experiments have shown that the variations in the tangential force and torque match the values obtained from the model.
- There is a considerable variation in the cutting forces for reaming with varying reamer sizes. The required torque is considerably less for reamers of small size. However, radial and axial forces are not having a significant effect on the variation of the size of the reamer.
- The changes in the dynamic forces are mainly found because of the cutting chip variation during the reaming process.
- During the steady-state reaming, the dynamic cutting force in tangential direction varies from 35 N to 50 N.
- The developed model could be applied to reaming process to minimize the defects caused, particularly while reaming the mild steel and aluminium materials using a 15, 20 and 24 mm reamer.
- The study could be further extended by researchers in this field for determining the effect of reaming on the defects in other metals, alloys and composites. Moreover, a possible extension is also to develop dynamic models by varying the reamer geometry and material.

## Conflict of interest

There are no conflicts to declare.

## Supporting information

Not applicable.

## References


[1] A. A. Bezerra, A. R. Machado, A. M. Souza, and E. O. Ezugwu, *J. Mater. Process. Technol.*, 2001, **112**, 185–198, doi: 10.1016/S0924-0136(01)00561-1.

[2] A. Monje, F. Monje-Gil, M. Burgueño, R. Gonzalez-Garcia, P. Galindo-Moreno, and H.-L. Wang, *Int. J. Periodontics Restor. Dent.*, 2016, **36**, 549–556, doi: 10.11607/prd.2525.

[3] E. Abele and N. Lautenschläger, *WT Werkstattstech*, 2017, **107**, 27–33.

[4] J. Fulemova and J. Rehor, *Ann. DAAAM Proc. Int. DAAAM Symp.*, 2016, **27**, 275–282.

[5] Y. Wang, X. Chen, and G. Liu, *Solid State Phenom.*, 2011, **175**, 321–325, doi: 10.4028/www.scientific.net/SSP.175.321.

[6] M. K. Das and S. A. Tobias, *Int. J. Mach. Tools Manuf.*, 1967, **7**, 63–89, doi: 10.1016/0020-7357(67)90026-1.

[7] Hindustan Machine Tools, Drilling and reaming, Production Technology, 1st ed., Bangalore, India, 2001, 147–159.

[8] O. Bhattacharyya, M. B. Jun, S. G. Kapoor, and R. E. DeVor, *Int. J. Mach. Tools Manuf.*, 2006, **46**, 1281–1290, doi: 10.1016/j.ijmachtools.2005.11.002.

[9] O. Bhattacharyya, S. G. Kapoor, and R. E. Devor, *Int. J. Mach. Tools Manuf.*, 2006, **46**, 836–846, doi: 10.1016/j.ijmachtools.2005.07.022.

[10] K. Sakuma and H. Kiyota, *J. Jpn. Soc. Precis. Eng.*, 1986, **20**, 103–108, doi: 10.2493/jjspe1933.48.745.

[11] M. E. Merchant, *Int. J. Appl. Phys.*, 1945, **16**, 267–275, doi: 10.1063/1.1707586.

[12] V. Chandrasekharan, S. G. Kapoor, and R. E. DeVro, *J. Manuf. Sci. Eng. Trans. ASME*, 1998, **120**, 563–570, doi: 10.1115/1.2830160.

[13] S. G. Kapoor, R. E. DeVor, R. Zhu, R. Gajjela, G. Parakkal, and D. Smithey, *Mach. Sci. Technol.*, 1998, **2**, 213–238, doi: 10.1080/10940349808945669.

[14] J. A. Yang, V. Jaganathan, and R. Du, *Int. J. Mach. Tools Manuf.*, 2002, **42**, 299–311, doi: 10.1016/S0890-6955(01)00102-X.

[15] P. V. Bayly, K. A. Young, S. G. Calvert, and J. E. Halley, *J. Manuf. Sci. Eng.*, 2001, **123**, 387–396, doi: 10.1115/1.1383551.

[16] M. Sajjadi and M. R. Movahhedy, ASME *Int. Mech. Eng. Congress Expo. Proc.*, 2008, **3**, 441–447, doi: 10.1115/IMECE2007-43028.

[17] X. H. Zhu and Y. J. Jia, *Tunn. Undergr. Space Technol.*, 2014, **41**, 255–262, doi: 10.1016/j.tust.2013.12.008.

[18] X. D. Wang, W. L. Ge, and Y. G. Wang, *Key Eng. Mater.*, 2018, **764**, 279–290, doi: 10.4028/www.scientific.net/KEM.764.279.

[19] C. Raghavendra Kamath and A. Kuttan, *Int. J. Mech. Prod. Eng. Res. Dev.*, 219, **9**, 931–938, doi: 10.24247/ijmperdoct201982.

[20] R. C. Kamath and A. K. K. Kuttan, *Maejo Int. J. Sci. Technol.*, 2009, **3**, 343–351.

[21] H. S. Kim and K. F. Ehmann, *Int. J. Mach. Tools Manuf.*, 1993, **33**, 651–673, doi: 10.1016/0890-6955(93)90099-G.

[22] E. L. Wilson, I. Farhoomand, and K. J. Bathe, *Earthq. Eng. Struct. Dyn.*, 1972, **1**, 241–252, doi: 10.1002/eqe.4290010305.

[23] A. Agic, M. Eynian, J. E. Ståhl, and T. Beno, *Int. J. Interact. Des.*, 2019, **13**, 557–565, doi: 10.1007/s12008-018-0513-5.

[24] A. Brandt, *Noise and Vibration Analysis: Signal Analysis and Experimental Procedures*. Chichester, UK: John Wiley & Sons, Ltd, 2011.

[25] J. A. Yang, V. Jaganathan, and R. Du, *Int. J. Mach. Tools Manuf.*, 2002, **42**, 299–311, doi: 10.1016/S0890-6955(01)00102-X.


© Engineered Science Publisher LLC 2021

[26] O. Bhattacharyya, M. B. Jun, S. G. Kapoor, and R. E. DeVor, *Int. J. Mach. Tools Manuf.*, 2006, **46**, 1281–1290, doi: 10.1016/j.ijmachtools.2005.11.002.

## Author information

***Dr. Raghavendra Kamath C****. is an Associate Professor at Department of Mechanical and Manufacturing, Manipal Institute of Technology, MAHE, Manipal, India. Machining of Metals; Non-conventional Machining; Modelling of Cutting Forces; Operations Research are the areas of his expertise.*

***Dr. Siddappa Bekinal*** *is an Associate Professor at Department of Mechanical and Manufacturing, Manipal Institute of Technology, MAHE, Manipal, India. Mechanical Vibrations; Rotor Dynamics; Turbomachinery are the areas of his expertise.*

***Mr. Ritesh Bhat*** *is an Assistant Professor at Department of Mechanical and Manufacturing, Manipal Institute of Technology, MAHE, Manipal, India. Machining of Materials, Lean Manufacturing, Design of Experiments, Optimization Techniques are the areas of his expertise.*

***Mr. Nithesh Naik*** *is an Assistant Professor at Department of Mechanical and Manufacturing, Manipal Institute of Technology, MAHE, Manipal, India. Machining of Materials; Machine Learning; Healthcare Informatics; Composite Materials; Finite Element Analysis are the areas of his expertise.*

***Dr. Appu Kuttan*** *is a Retd. Professor, Department of Mechanical Engineering, National Institute of Technology, Surathkal, Karnataka. He recieved his Ph D from IIT Madras and has several years of teaching experience both at the undergraduate and postgraduate levels.*

**Publisher's Note:** Engineered Science Publisher remains neutral with regard to jurisdictional claims in published maps and institutional affiliations.

 © Engineered Science Publisher LLC 2021